STEM CELLS AND DEVELOPMENT
Volume 18, Number 5, 2009

DOI: 10.1089/scd.2008.0253

SEMINAL REPORT

Pulmonary Passage is a Major Obstacle for Intravenous Stem Cell Delivery: The Pulmonary First-Pass Effect

Uwe M. Fischer,[1,3] Matthew T. Harting,[1] Fernando Jimenez,[1] Werner O. Monzon-Posadas,[1] Hasen Xue,[1] Sean I. Savitz,[2] Glen A. Laine,[3] and Charles S. Cox, Jr.[1,3]

Intravenous (IV) stem cell delivery for regenerative tissue therapy has been increasingly used in both experimental and clinical trials. However, recent data suggest that the majority of administered stem cells are initially trapped in the lungs. We sought to investigate variables that may affect this pulmonary first-pass effect. In anesthetized Sprague-Dawley rats, silicone tubing catheters were placed in the left internal jugular vein and common carotid artery. We investigated four different cell types: mesenchymal stromal cells (MSC), multipotent adult progenitor cells (MAPCs), bone marrow–derived mononuclear cells (BMMC), and neural stem cells (NSC). Cells were co-labeled with Qtracker® 655 (for flow cytometry) and Qtracker® 800 (for infrared imaging) and infused intravenously with continual arterial sample collection. Samples were analyzed via flow cytometry to detect labeled cells reaching the arterial circulation. Following sampling and exsanguination, heart, lungs, spleen, kidney, and liver were harvested and placed on an infrared imaging system to identify the presence of labeled cells. The majority of MSCs were trapped inside the lungs following intravenous infusion. NSC and MAPC pulmonary passage was 2-fold and BMMC passage was 30-fold increased as compared to MSCs. Inhibition of MSC CD49d significantly increased MSC pulmonary passage. Infusion via two boluses increased pulmonary MSC passage as compared to single bolus administration. Infrared imaging revealed stem cells evenly distributed over all lung fields. Larger stem and progenitor cells are initially trapped inside the lungs following intravenous administration with a therapeutically questionable number of cells reaching the arterial system acutely.

Introduction

Stem cell–based regenerative strategies for mesenchymal tissue injuries hold promise. One challenge associated with this therapeutic approach is the route of administration for efficient stem cell delivery. Cardiac tissue repair has been approached using intracoronary, systemic, and direct myocardial stem cell injection [1–3]. However, for stem cell delivery to other organs such as the brain, systemic administration may be preferable. In addition, strategies for local stem cell delivery increase risks and side effects such as bleeding and tissue injury with direct tissue injection or occlusion and embolization associated with direct arterial administration [1–3]. Therefore, if stem cell therapy is to be broadly applied as a therapeutic strategy, a simple intravenous (IV) approach would be ideal, given broad biodistribution and easy access. Consequently, intravenous infusion has been used as the route of cell delivery for a large number of preclinical studies [4–6] and is the route of delivery for some early clinical trials [7,8]. However, questions have been raised regarding the ability to obtain a critical number of cells to the area of injury with a systemic intravenous approach [9–11]. Previous studies from our laboratory using intravenous administration of mesenchymal stromal cells (MSCs) for regenerative therapy of rat brain injuries demonstrate that few MSCs reach the area of injury, and the vast majority of administered cells are trapped inside the lungs. In addition, Schrepfer et al. showed in a mouse model that within seconds after MSC intravenous injection, the majority of cells were found in the lungs, and they suggested that cell size was a key factor in this phenomenon [11].

To further address this issue, we performed studies evaluating stem cell passage across the pulmonary circulation

[1]Department of Pediatric Surgery and [2]Department of Neurology, University of Texas Medical School at Houston, Houston, Texas.
[3]Michael E. DeBakey Institute for Comparative Cardiovascular Science and Biomedical Devices, Texas A&M University, College Station, Texas.

depending on variables such as the number, mode, and type of stem cell IV administration.

Materials and Methods

All procedures were approved by the University of Texas Animal Welfare Committee and are consistent with the National Institutes of Health "Guide for the Care and Use of Laboratory Animals" (NIH publication 85-23, revised 1985). All cells used in our experiments were of rat origin.

Isolation, characterization, and labeling of rat MSCs

We isolated MSCs from the bone marrow of Sprague-Dawley rats. MSCs were expanded on a fibronectin matrix, in MAPC media as previously described [12]. Flow cytometric immunophenotyping was used to ensure that the MSCs are: $CD11b^-$, $CD45^-$, $CD29^+$, $CD49e^+$, $CD73^+$, $CD90^+$, $CD105^+$, and $Stro\text{-}1^+$. Additionally, multilineage potential was confirmed via differentiation to chondrocytes, adipocytes, and osteocytes. MSCs were co-labeled for immunohistochemistry and flow cytometric detection of intra-arterial (IA) sampling using Qtracker® 525 and Qtracker® 655 labeling kits (Invitrogen, Carlsbad, CA). Qtracker® 700 and Qtracker® 800 cell labeling kits (Invitrogen, Carlsbad, CA) were used for detection of MSCs using the Odyssey® infrared imaging system. MSCs were labeled per the manufacturer's protocol. Briefly, cells and the fluorescent Qdot® nanocrystal mixture were suspended in MAPC media and incubated in the dark at 37°C for 2 h. The percentage of cells effectively labeled was determined via flow cytometry and was consistently >95%. MSCs were passaged no more than four times.

Expansion and labeling of rat BMMCs, NSCs, and MAPCs

BMMCs and neural stem cells (NSCs) were isolated as previously described [12,13]. Multipotent adult progenitor cells (MAPC) were provided by Yuehua Jiang, PhD at the University of Minnesota Stem Cell Institute. MAPCs were reanimated and expanded on fibronectin matrix.

Cells were co-labeled with Qtracker® 655 (immunohistochemistry and flow cytometry of IA sampling) and Qtracker® 800 (Odyssey® infrared imaging) using a cell labeling kit (Invitrogen, Carlsbad, CA), per the manufacturer's protocol. Briefly, cells suspended in MAPC media were incubated for 2 h in the dark at 37°C with fluorescent Qdot® nanocrystals. The percentage of cells effectively labeled was determined via flow cytometry and was consistently >95%. MAPCs were expanded no more that two times.

Cell size determination

A Coulter Counter Z1 Series particle counter (Beckman Coulter Inc., Hialeah, FL) was used to determine the size range of our cell populations. Prior to taking measurements, we optimized, using the "Trough Finding" method, the dynamic range of size measurement by adjusting gain and current specified in the Beckman Counter Z1 Series user manual. Briefly, the range of the cell size was estimated, using dual threshold, by setting the upper threshold as 1.5 times the optimized gain and current settings and the lower threshold as half the optimized settings. We determined the distribution of cell sizes by recording the total particle count within a range of increasing specific volume (μm^3) limits. We distinguished the cell population from debris by observing the generated minima on both sides of the curve. We simultaneously verified the cell counts using a hemocytometer. The percent of total particle counts versus cell volume was plotted using Microsoft Excel (Fig. 1). We then calculated the diameter based on cell volume.

Intravenous cell infusion with intra-arterial sampling

Cells were labeled with Qtracker® 655 and Qtracker® 800 as described earlier. Rats were anesthetized with 4% isoflurane and O_2 inhalation and spontaneously breathing. The left internal jugular vein was exposed, and a silicone tubing catheter (ID: 0.635 mm; OD: 1.19 mm) was inserted. The MSCs were infused in 1 mL of phosphate-buffered saline (PBS) vehicle, with a 1-mL catheter flush to ensure that all cells were infused. IA cannulation of the left common carotid artery was achieved (same size catheter as IV). Rats were heparinized at 100u/kg (~25u/rat). Control IA samples were collected (250 µL/sample) prior to infusion. Cell infusion was initiated with continual IA sample collection until ~10 min after completion of infusion (~30–40 samples total at 250 µL/sample). Samples were then analyzed via flow cytometry (BD LSR II; BD Biosciences, San Jose, CA) to detect labeled cells reaching the arterial circulation.

Experimental protocol/groups

Experimental groups are summarized in Table 1. All groups except group B cells were intravenously administered in one bolus (2×10^6 cells). In group B we injected MSCs (4×10^6 cells total) via two equal boluses (2×10^6 cells each). In groups A–G we used MSCs from passage five except for group C where we used passage one MSCs. In groups D–G, we either pretreated MSCs with the poloxamer 188 (P188, a purified nonionic block copolymer chemical surfactant, provided by Robert Hunter, MD, PhD, Department of Molecular Pathology, University of Texas Medical School at Houston, TX) (D), an anti-P-selectin antibody (40 µg/mL; Santa Cruz Biotechnology, Santa Cruz, CA) (E), anti-VCAM-1 antibody (40 µg/mL; Santa Cruz Biotechnology, Santa Cruz, CA) or by incubation of MSC prior to infusion with anti-CD49d antibody (10 µg/mL; BioLegend, San Diego, CA) (F). To assess for the impact of different cell types and sizes on pulmonary passage, we additionally used MAPC, bone marrow–derived mononuclear cells (BMMC), and NSC (groups H–J), respectively.

Identification of infused cells versus rat blood

Labeled stem cells were identified in the arterial blood samples using flow cytometry. The flow cytometric scatter for MSCs is shown in Figure 2 with rat whole blood cells (A) and Qtracker®-labeled MSCs (B). A histogram overlay of the whole blood (gray) and MSC (white) population is shown (C). The red line shows the positive threshold (10^2) used to distinguish infused MSCs from other cells (>90% of MSCs). The clear difference in intensity of rat blood (A) versus MSCs (B) allows recognition of infused cells by flow cytometry. Also, a representative dual parameter dot plot identifying cells that transverse the lungs in vivo is shown (D).

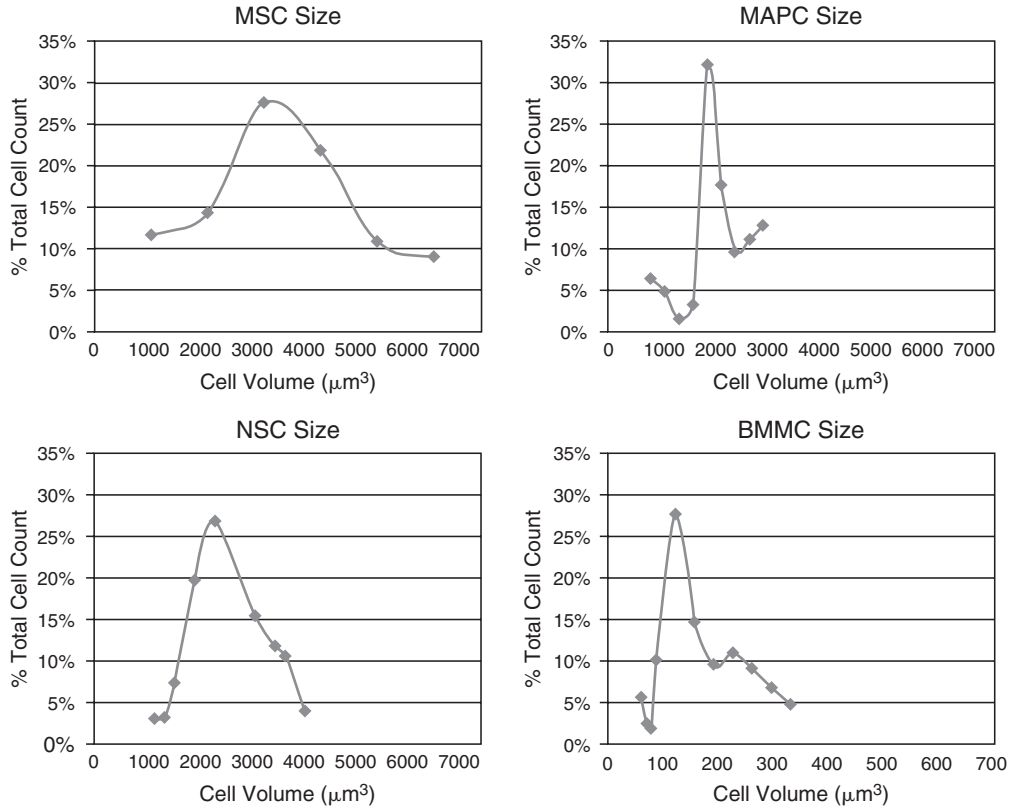

FIG. 1. A Coulter Counter Z1 Series particle counter (Beckman Coulter Inc., Hialeah, FL) was used to determine the size range of our cell populations. Prior to taking measurements, we optimized the dynamic range of size measurement by adjusting gain and current settings using methods specified in the Beckman Counter Z1 Series user manual. The distribution of cell sizes was determined by recording the total particle count within a range of increasing specific volume (μm^3) limits. Cell population was distinguished from debris by observing the generated minima on both sides of the curve. Abbreviations: MSC, mesenchymal stem cell; MAPC, multipotent adult progenitor cell; NSC, neural stem cell; BMMC, mononuclear cell fraction.

Infrared macroscopic cell tracking

At the end of each experiment, lung, heart, spleen, kidney, and liver tissue were collected and placed on the Odyssey® 2.1 infrared imaging system (LI-COR Biosciences, Lincoln, Nebraska) and imaged to identify the presence of the labeled cells. Tissues were imaged at 800 nm wavelength, with a resolution of 84 μm, and a focus offset of 1 mm.

Table 1. Experimental Groups

Group	*Cell type*	*Number*	*Bolus*	*Modifications*	*n*
A	MSC	2×10^6	One	None	5
B	MSC	4×10^6	Two	None	5
C	MSC	2×10^6	One	Passage one	4
D	MSC	2×10^6	One	P188 treatment	5
E	MSC	2×10^6	One	P-selectin antibody	5
F	MSC	2×10^6	One	VCAM-1 antibody	5
G	MSC	2×10^6	One	CD49d	2
H	MAPC	2×10^6	One	None	5
I	BMMC	2×10^6	One	None	5
J	NSC	2×10^6	One	None	5

Abbreviations: MSC, mesenchymal stem cells; MAPC, multipotent adult progenitor cells; BMMC, bone marrow–derived mononuclear cells; NSC, neural stem cells; P188, polyoxamer 188; P-selectin, animal pretreatment with anti-P-selectin antibody; VCAM-1, animal pretreatment with anti-VCAM-1 antibody; CD49d, MSC pretreatment with anti-CD49d antibody.

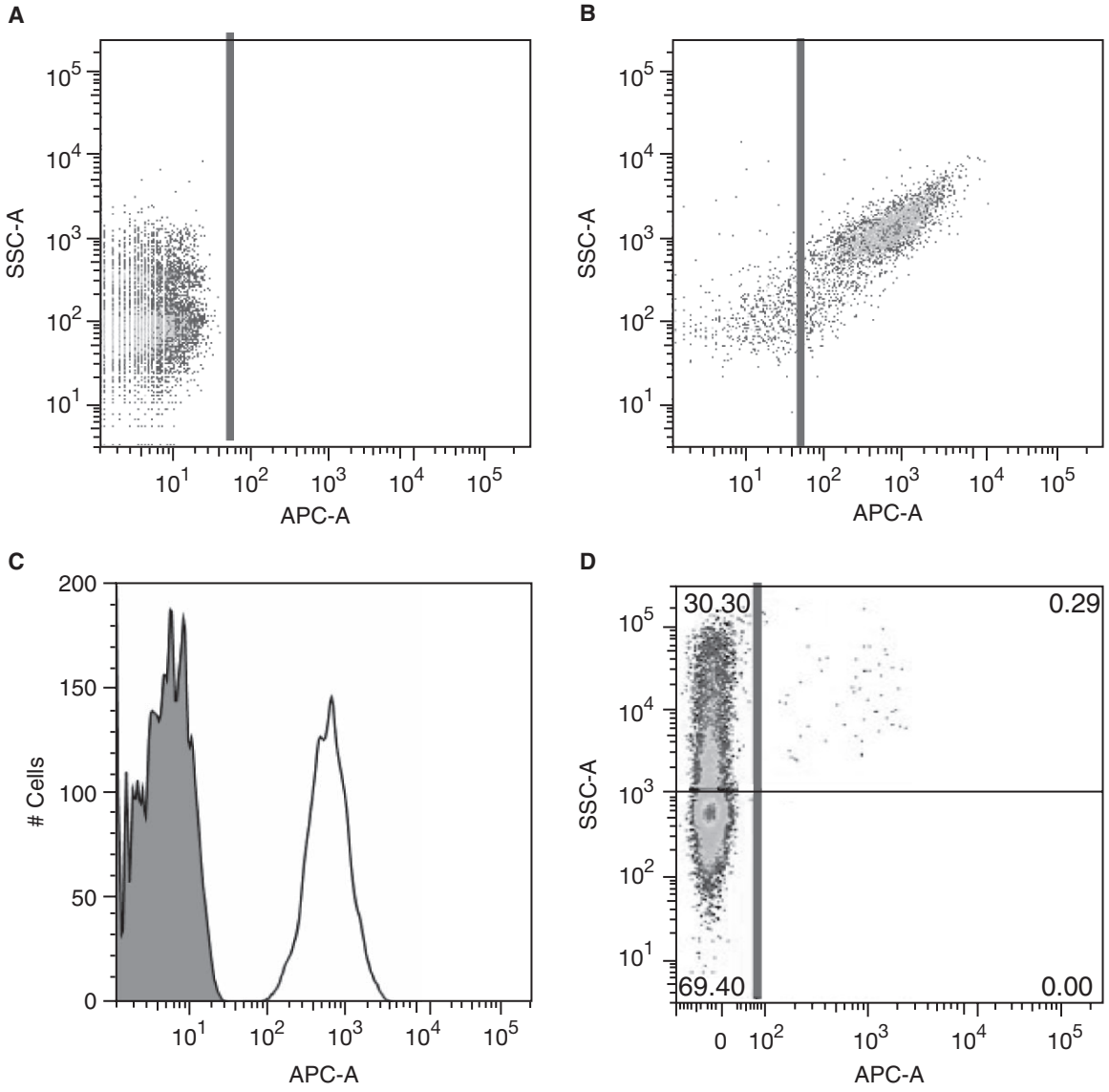

FIG. 2. Labeled MSCs were identified in the arterial blood samples using flow cytometry. The flow cytometric dual parameter dot plots show rat whole blood cells (**A**) and Qtracker®-labeled MSCs (**B**). The *y*-axis is side scatter (SSC) and the *x*-axis is the channel (APC) in which the Qtracker® can be detected. A histogram overlay of the whole blood (gray) and MSC (white) population is shown (**C**). A representative dual parameter dot plot identifying cells that transverse the lungs in vivo (**D**). The vertical line shows the positive threshold (10^2) used to distinguish infused MSCs from other cells (>90% of MSCs). The clear difference in intensity of rat blood (**A**) versus MSCs (**B**) allows recognition of infused cells by flow cytometry.

Statistical analyses

Data are presented as mean ± standard error. Data were analyzed using Student's *t*-test and ANOVA with Tukey's test for post-hoc analysis. A P value of <0.05 was considered statistically significant.

Results

Figure 3 depicts the total number (A) and percentage (B) of stem cells reaching the carotid artery, respectively. According to the percentages of stem cells reaching the carotid artery (Fig. 3B) intravenous infusion of MSCs via two boluses (B), pretreatment of MSCs with anti-CD49d antibody (G), and IV infusion of MAPCs (H), BMMCs (I), and NSCs (J) resulted in a significant increase in pulmonary stem cell passage compared to a single MSC bolus injection (A) (P = 0.01, 0.02, 0.04, 0.0003, and 0.02, respectively).

The time course of cell numbers collected from the arterial line is shown in Figure 4. Except for groups B and I, the majority of stem cells reached the arterial system during the first 2 min (~10 samples) following intravenous infusion. While in group B stem cells were infused via two boluses, group I consisted of a single bolus administration of MSCs resulting in two sampling peaks.

Figure 5 depicts representative infrared macroscopic cell tracking images of all experimental groups. Except for BMMCs, a clear signal can be seen in the lungs of all

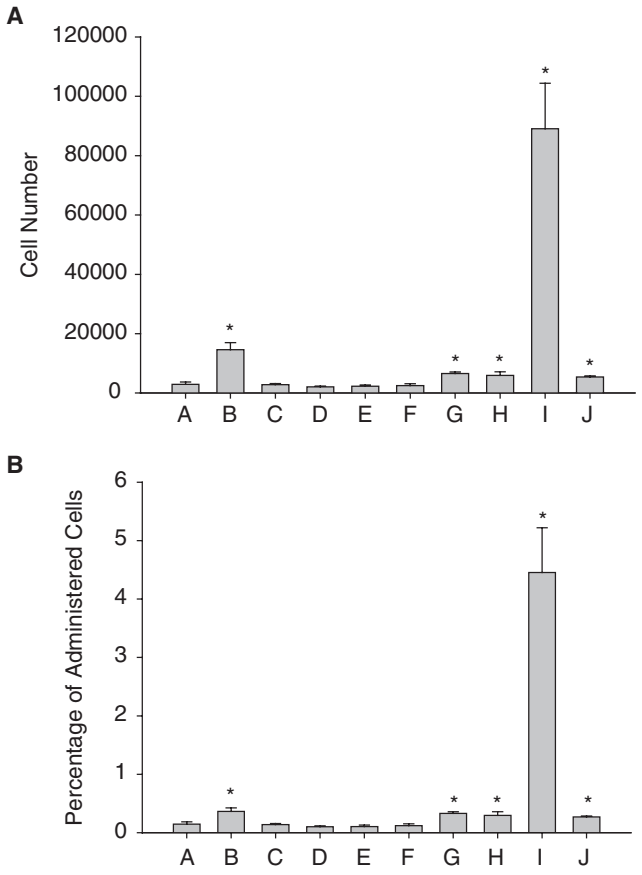

FIG. 3. Pulmonary stem cell passage. Total number (**A**) and percentage (**B**) of stem cells reaching the carotid artery are shown for groups A–J. *$P < 0.05$ versus A.

groups demonstrating the majority of infused stem cells to be trapped inside the pulmonary system. In groups G, H, I, and J, fluorescence intensity is lower reflecting a smaller number of cells trapped inside the lungs. However, cells could not be detected in any of the other organs, in none of the groups.

Intravenous injection of two MSC boluses (2 million each) labeled with two different colors is shown in Figure 6. The infrared imaging shows an even distribution of the first bolus MSCs (green) and a distinct pattern of the second bolus (red) mainly located in the central pulmonary vasculature (A). The total number of stem cells reaching the carotid artery was significantly higher for bolus 2 compared to bolus 1 (B). The distribution of the number of MSCs per sample is shown for both bolus 1 (black) and bolus 2 (white).

Discussion

Our data show that following intravenous infusion, the majority of stem cells are trapped inside the lungs. MSC infusion with two boluses and blocking of MSC CD49d as well as infusion of MAPCs and NSCs resulted in a small but significant increase in stem cell passage across the pulmonary microvascular barrier. Infusion of BMMCs, however, resulted in a 30-fold pulmonary passage increase as compared to a single MSC bolus.

We and others have shown that intravenous infusion of stem cells does not yield a large number of cells reaching the organ of interest primarily due to the majority of stem cells being trapped inside the lungs [9–11]. In an effort to increase the number of stem cells crossing over to the arterial circulation, we analyzed several experimental groups focusing on cell size and adhesion molecules as potential variables.

We first hypothesized that cell size would play a crucial role in pulmonary capillary passage. Our hypothesis is based on a study from Schrepfer et al., which showed that smaller microspheres (4–5 μm) can pass through the pulmonary system while the majority of 20 μm microspheres and MSCs (15–19 μm) are trapped inside the lungs. Furthermore, treatment of the animals with sodium nitroprusside for vasodilation resulted in an increased pulmonary passage [11]. We, therefore, compared pulmonary passage of MSCs, MAPCs, NSCs, and BMMCs (with average diameters: 18, 15, 16, and 7 μm, respectively). While BMMC pulmonary passage was 30-fold higher compared to MSCs, MAPC, and NSC passage was only 2-fold increased. The marked increase for BMMCs supports the findings from Schrepfer and colleagues showing increased pulmonary passage of small (4–5 μm) compared to large (20 μm) microspheres. Although MSC, MAPC, and NSC sizes in our study were within the size range reported by Schrepfer et al. (15–19 μm), we found a significant 2-fold increase in pulmonary passage for MAPCs and NSCs compared to MSCs. In addition, BMMCs differ from MSCs not only in size but also regarding their adhesion abilities. Thus, we concluded that factors other than cell size such as adhesion to the vascular endothelium may also be involved in pulmonary cell trapping. This hypothesis is supported by a recent study from Ruster and colleagues suggesting that P-selectin and a counter-ligand are involved in the adhesion and extravasation of MSCs [14]. They demonstrated that MSCs interact with endothelial cells in a coordinated fashion under shear flow, engaging both P-selectin and VCAM-1/VLA-4 [14]. Ruster et al. used human MSCs for their experiments. However, the counter-ligands for both P-selectin and VCAM-1/VLA-4 have also been found on MSCs of rat origin published by Wang et al. [15].

While pretreatment of animals with anti-P-selectin or anti-VCAM-1 antibodies in our study did not change pulmonary MSC passage, inactivation of the VCAM-1 counter-ligand on the MSC surface (VLA-4/CD49d) resulted in a significant increase of MSCs reaching the arterial system. We therefore conclude that VCAM-1 rather than P-selectin is involved in MSC adhesion to the pulmonary vasculature endothelium. Furthermore, in our study, the administration of 4×10^6 MSCs via two boluses significantly increased pulmonary passage. We believe this further supports the hypothesis that there is a component of receptor-mediated pulmonary MSC entrapment as the number of MSCs given during the second bolus was significantly higher as compared to the first bolus suggesting saturation of receptors during the first bolus allowing more cells to pass the vasculature with the second bolus. In addition to vascular adhesion molecule interaction with stem cells, cell type–specific deformability might also be involved in pulmonary stem cell passage. Although our data do not allow us to further speculate on this issue, Wiggs et al. demonstrated the impact of capillary pathway size and neutrophil deformability on neutrophil transit through rabbit lungs [16]. Therefore, the

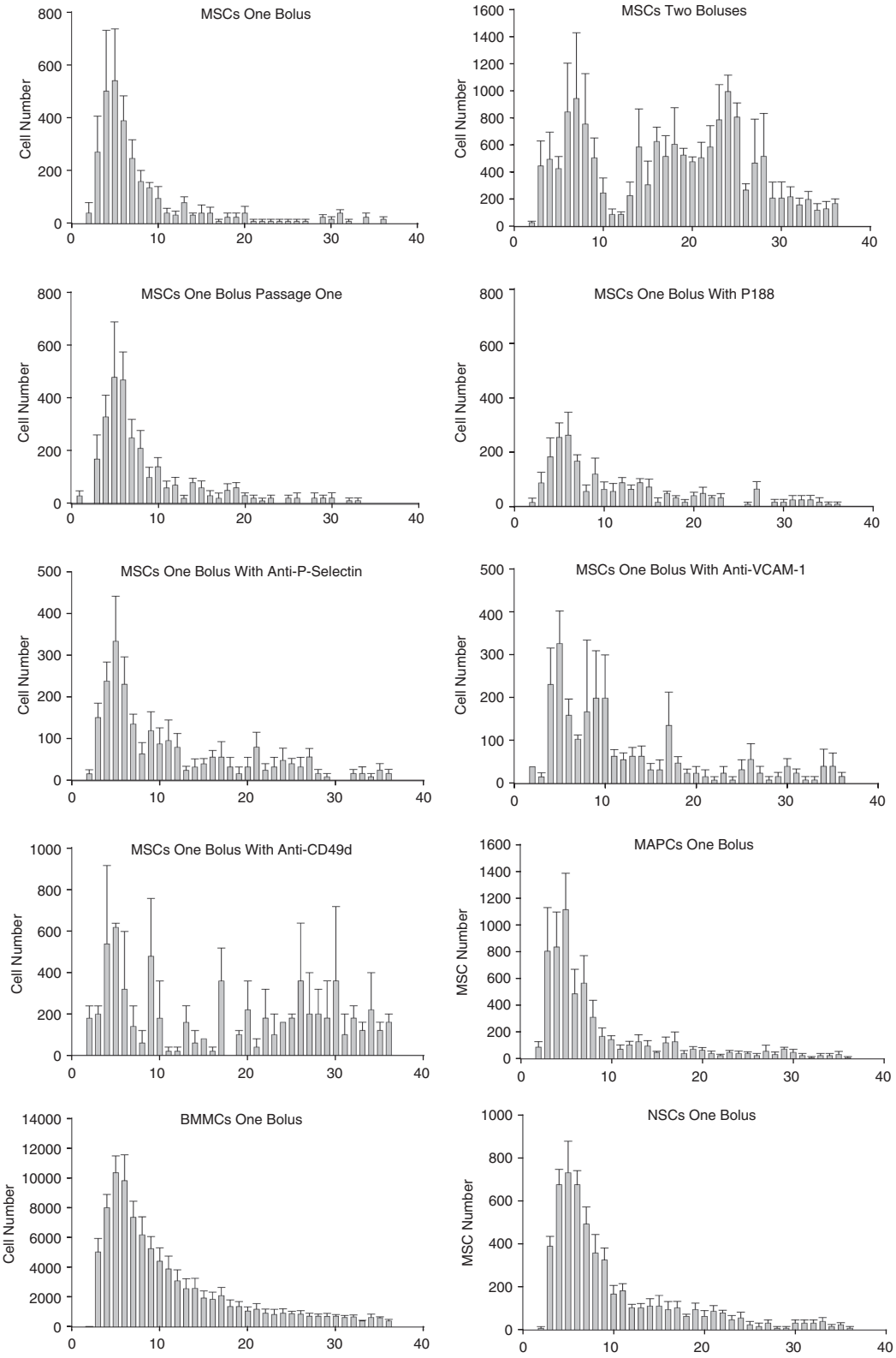

FIG. 4. Intra-arterial (IA) MSC collection after intravenous (IV) infusion ($n = 5$ rats/group). Stem cells (Qtracker®-labeled) were infused via the internal jugular vein and blood was continuously sampled from the common carotid artery over the subsequent 10 min (35–40 samples). IA blood samples were run through a flow cytometer to detect the Qtracker®-labeled stem cells. Number of MSCs per sample is shown on the *y*-axis and sample numbers are shown on the *x*-axis.

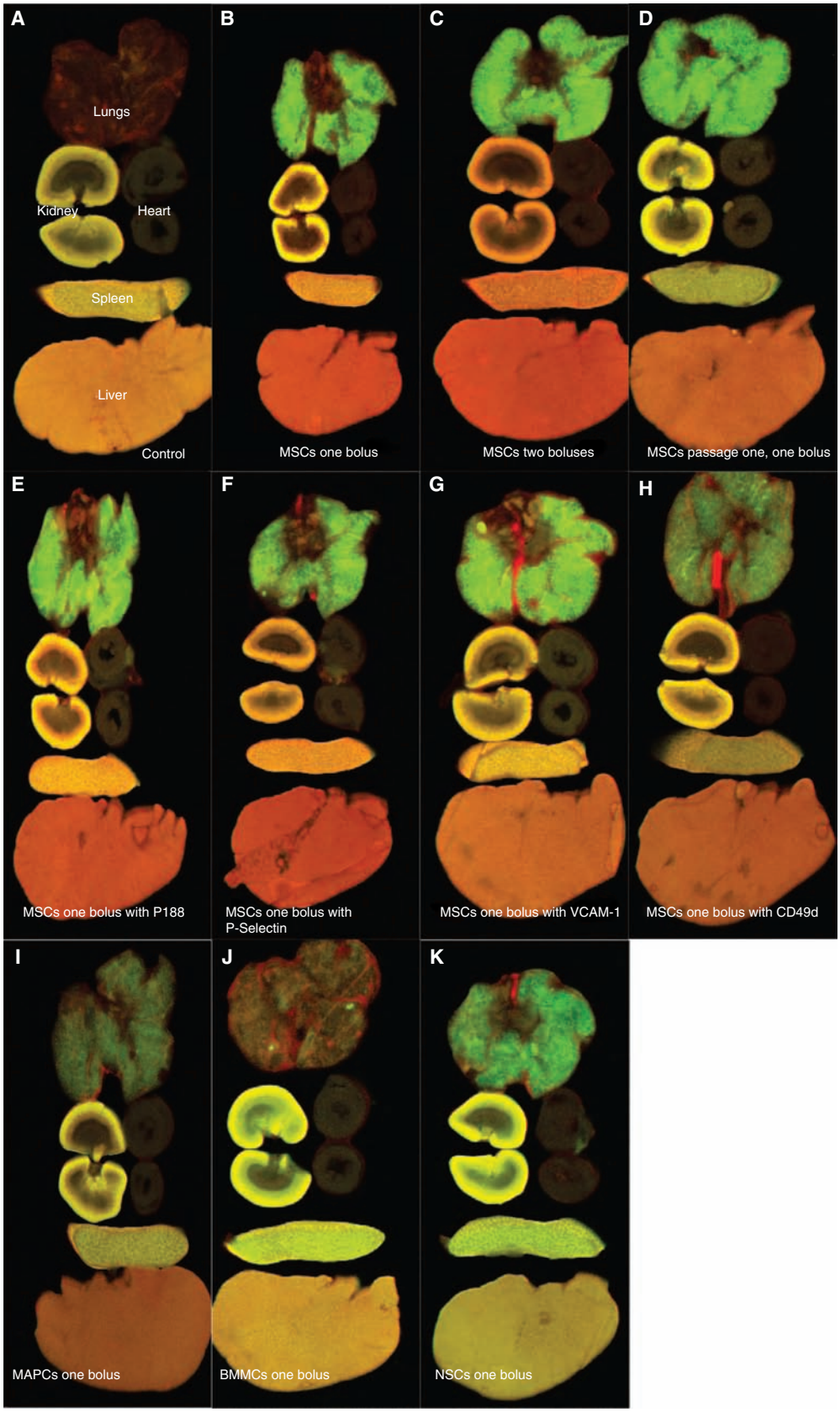

FIG. 5. Infrared imaging of organs immediately after intravenous stem cell infusion. Lungs, heart, kidney, spleen, and liver of rats immediately after intravenous stem cell infusion (**B**–**K**) or vehicle (**A**, control) imaged ex vivo on the LI-COR Odyssey® infrared imaging system.

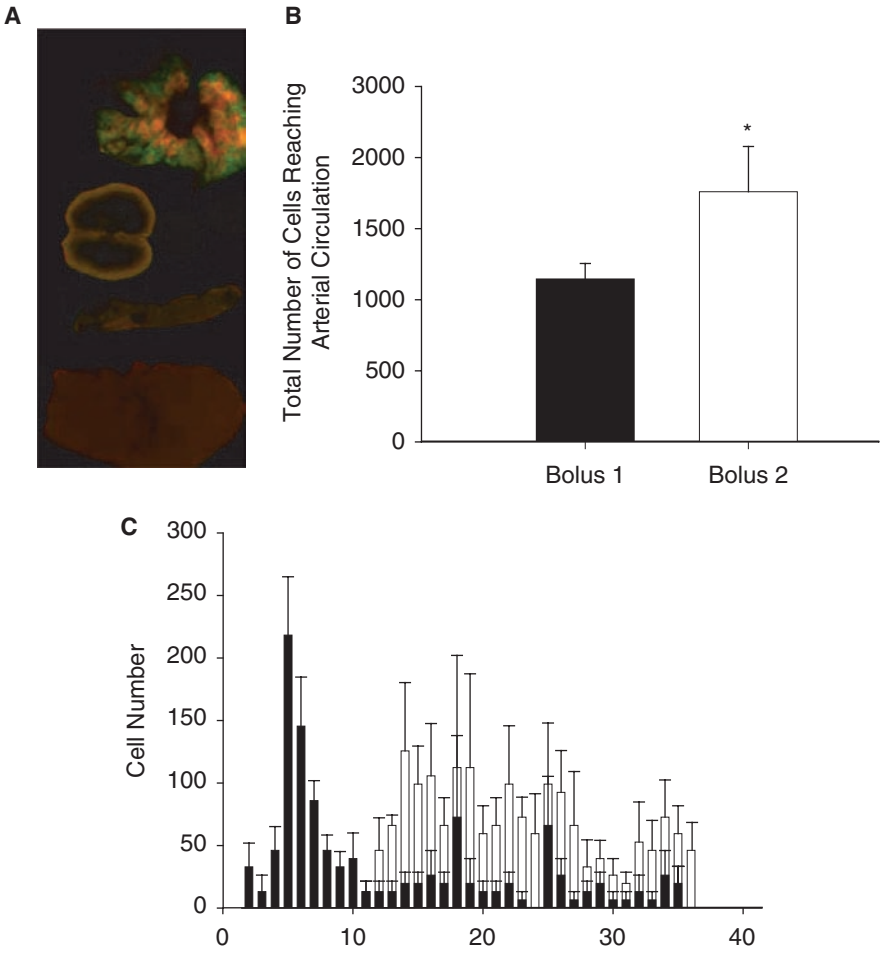

FIG. 6. Intravenous injection of two MSC boluses (2 million each) labeled with two different colors. Infrared imaging of lungs, heart, kidney, spleen, and liver immediately after intravenous stem cell infusion (**A**), total number of stem cells reaching the carotid artery for bolus 1 and bolus 2, respectively (**B**), and number of MSCs per sample is shown (**C**; see Fig. 4 for details). *$P < 0.05$ versus bolus 1.

deformability potential of different cell types and its effect on pulmonary passage will have to be considered in future studies.

We found significantly increased pulmonary passage of BMMCs and NSCs as compared to MSCs. Both BMMCs and NSCs express CD49d, which conflicts with our hypothesis of CD49d/VCAM-1-mediated cell adhesion. However, despite potential binding to VCAM-1 via CD49d, BMMCs and NSCs might have advantages over MSCs due to their smaller size that could explain improved pulmonary passage. Hence, we conclude that the combined effect of cell size and adhesion molecule expression is crucial for stem and progenitor cell passage through the pulmonary microvasculature.

Our findings of intravenously injected stem cells initially being trapped in the lungs are supported by studies from other groups [9,10,17,18]. While our study focused on mechanisms involved in pulmonary entrapment, these studies investigated stem cell redistribution from the lungs. In rodents, intravenously injected MSCs or peripheral blood stem cells (PBSCs) accumulated initially in the lungs, and gradually moved to liver, spleen, kidney, and bone marrow within 48 h [9,10]. Rochefort et al. found a 50–60% pulmonary accumulation of MSCs 1 h after the injection with subsequent decrease to about 30% 3 h postinjection [18]. In humans, intravenously injected PBSCs also showed a high lung uptake at 30 min [17]. Four hours after the injection, distributions of PBSCs were 42.12% in spleen, 21.3% in liver, and only 5.8% in lung [17]. These studies suggest that pulmonary trapping of stem cells following intravenous administration is only a transient phenomenon. However, redistribution of stem cells showed the majority of stem cells in liver and spleen to an extent that does not reflect the actual percentage of cardiac output. Thus, we believe that initial pulmonary trapping of stem cells might alter their ability for tissue homing leading to nonspecific accumulation especially in the reticuloendothelial system.

Taken together, we present evidence that pulmonary passage is a major obstacle for systemic intravenous stem cell administration with smaller number of stem cells crossing over to the arterial system and the majority of cells being trapped inside the lungs. Both cell size and receptor-mediated adhesion and/or stem cell type appear to be crucial variables for pulmonary stem cells passage. Modification of these variables results in significantly increased pulmonary stem cell passage. However, although significantly higher, the number of cells reaching the arterial circulation still represents only a small fraction of the originally administered amount. As efficient intravenous stem cell therapy requires a sufficient number of stem cells reaching the target organ, it is crucial to increase the number of stem cells reaching the arterial circulation. Apart from increasing the number of cells reaching the arterial circulation, the effects of those cells trapped inside the lungs have to be further evaluated, as recent studies have shown that MSCs residing in the lungs may cause tissue damage [19]. In addition, recent studies from Coyne et al. have demonstrated that intrinsic characteristics

of MSC transplanted into adults rat brains stimulated a host inflammation resulting in acute rejection of the implanted cells [20,21]. An immune response might also be responsible for the pulmonary tissue damage observed by Anjos-Afonso et al. [19]. Due to the acute nature of our study we did not assess for an immune response following stem cell administration. However, future studies evaluating the long-term effect of stem cells following intravenous administration will have to include analysis of immune response to stem cells residing in the pulmonary tissue.

Limitations of this study

As we focused on factors involved in early pulmonary entrapment, we can only comment on the short-term course of intravenously administered stem cells. Consequently, it is not possible to determine the ultimate cell fate such as delayed release from the pulmonary vasculature and further arterial distribution. Furthermore, we cannot demonstrate the long-term effect of stem cell marker and/or receptor manipulation, although beneficial for pulmonary passage, on homing to the target tissue.

Funding Sources

T32 GM 068792-06, M01 RR 02558, R21 HD 042659-01A1, Children's Memorial Hermann Foundation, Texas Higher Education Coordinating Board. Dr. Fischer is a Feodor-Lynen Fellow with the Alexander-von-Humboldt Foundation.

Author Disclosure Statement

None.

References

1. Dimmeler S, J Burchfield and AM Zeiher. Cell-based therapy of myocardial infarction. Arterioscler Thromb Vasc Biol February 2008;28:208–216.
2. Ott HC, J McCue and DA Taylor. Cell-based cardiovascular repair—the hurdles and the opportunities. Basic Res Cardiol November 2005;100:504–517.
3. Sherman W, TP Martens, JF Viles-Gonzalez and T Siminiak. Catheter-based delivery of cells to the heart. Nat Clin Pract March 2006;3:S57–S64.
4. Mahmood A, D Lu and M Chopp. Marrow stromal cell transplantation after traumatic brain injury promotes cellular proliferation within the brain. Neurosurgery November 2004;55: 1185–1193.
5. Ukai R, O Honmou, K Harada, K Houkin, H Hamada and JD Kocsis. Mesenchymal stem cells derived from peripheral blood protects against ischemia. J Neurotrauma March 2007;24:508–520.
6. Krause U, C Harter, A Seckinger, D Wolf, A Reinhard, F Bea, T Dengler, S Hardt, A Ho, HA Katus, H Kuecherer and A Hansen. Intravenous delivery of autologous mesenchymal stem cells limits infarct size and improves left ventricular function in the infarcted porcine heart. Stem Cells Dev February 2007;16:31–37.
7. Horwitz EM, DJ Prockop, LA Fitzpatrick, WW Koo, PL Gordon, M Neel, M Sussman, P Orchard, JC Marx, RE Pyeritz and MK Brenner. Transplantability and therapeutic effects of bone marrow-derived mesenchymal cells in children with osteogenesis imperfecta. Nat Med March 1999;5:309–313.
8. Lazarus HM, SE Haynesworth, SL Gerson, NS Rosenthal and AI Caplan. Ex vivo expansion and subsequent infusion of human bone marrow-derived stromal progenitor cells (mesenchymal progenitor cells): implications for therapeutic use. Bone Marrow Transplant October 1995;16:557–564.
9. Gao J, JE Dennis, RF Muzic, M Lundberg and AI Caplan. The dynamic in vivo distribution of bone marrow-derived mesenchymal stem cells after infusion. Cells Tissues organs 2001;169:12–20.
10. Daldrup-Link HE, M Rudelius, S Metz, G Piontek, B Pichler, M Settles, U Heinzmann, J Schlegel, RA Oostendorp and EJ Rummeny. Cell tracking with gadophrin-2: a bifunctional contrast agent for MR imaging, optical imaging, and fluorescence microscopy. Eur J Nucl Med Mol Imaging September 2004;31:1312–1321.
11. Schrepfer S, T Deuse, H Reichenspurner, MP Fischbein, RC Robbins and MP Pelletier. Stem cell transplantation: the lung barrier. Transplant Proc March 2007;39:573–576.
12. Harting M, F Jimenez, S Pati, J Baumgartner and C Cox, Jr. Immunophenotype characterization of rat mesenchymal stromal cells. Cytotherapy 2008;10:243–253.
13. Davis AA and S Temple. A self-renewing multipotential stem cell in embryonic rat cerebral cortex. Nature November 17, 1994;372:263–266.
14. Ruster B, S Gottig, RJ Ludwig, R Bistrian, S Muller, E Seifried, J Gille and R Henschler. Mesenchymal stem cells display coordinated rolling and adhesion behavior on endothelial cells. Blood December 1, 2006;108:3938–3944.
15. Wang C, Y Xu, WG Song and WS Chang. [Isolation and culturation, phenotype detection of rat bone marrow mesenchymal stem cells]. Xi bao yu fen zi mian yi xue za zhi = Chinese J Cell Mol Immunol May 2007;23:466–468.
16. Wiggs BR, D English, WM Quinlan, NA Doyle, JC Hogg and CM Doerschuk. Contributions of capillary pathway size and neutrophil deformability to neutrophil transit through rabbit lungs. J Appl Physiol July 1994;77:463–470.
17. Kang WJ, HJ Kang, HS Kim, JK Chung, MC Lee and DS Lee. Tissue distribution of 18F-FDG-labeled peripheral hematopoietic stem cells after intracoronary administration in patients with myocardial infarction. J Nucl Med August 2006;47: 1295–1301.
18. Rochefort GY, P Vaudin, N Bonnet, JC Pages, J Domenech, P Charbord and V Eder. Influence of hypoxia on the domiciliation of mesenchymal stem cells after infusion into rats: possibilities of targeting pulmonary artery remodeling via cells therapies? Respir Res 2005;6:125.
19. Anjos-Afonso F, EK Siapati and D Bonnet. In vivo contribution of murine mesenchymal stem cells into multiple cell-types under minimal damage conditions. J Cell Sci November 1, 2004;117:5655–5664.
20. Coyne TM, AJ Marcus, K Reynolds, IB Black and D Woodbury. Disparate host response and donor survival after the transplantation of mesenchymal or neuroectodermal cells to the intact rodent brain. Transplantation December 15, 2007;84:1507–1516.
21. Coyne TM, AJ Marcus, D Woodbury and IB Black. Marrow stromal cells transplanted to the adult brain are rejected by an inflammatory response and transfer donor labels to host neurons and glia. Stem Cells (Dayton, Ohio) Nov 2006;24:2483–2492.

Address reprint requests to:
Dr. Charles S. Cox, Jr.
Department of Pediatric Surgery
University of Texas Medical School at Houston
6431 Fannin Street, Suite 5.236
Houston, TX 77030

E-mail: Charles.S.Cox@uth.tmc.edu

Received for publication August 24, 2008
Accepted after revision December 19, 2008
Prepublished on Liebert Instant Online December 19, 2008